



Spatial differences in dissolved silicon utilization in Lake Baikal, Siberia: Examining the impact of high diatom biomass events and eutrophication

V. N. Panizzo ^{1,2*} S. Roberts,^{1,2} G. E. A. Swann ^{1,2} S. McGowan ^{1,2} A. W. Mackay,³ E. Vologina,⁴ V. Pashley,⁵ M. S. A. Horstwood⁵

¹School of Geography, University of Nottingham, Nottingham, UK

²Centre for Environmental Geochemistry, University of Nottingham, Nottingham, UK

³Environmental Change Research Centre, Department of Geography, University College London, London, UK

⁴Institute of Earth's Crust, Siberian Branch of the Russian Academy of Sciences, Irkutsk, Russia

⁵NERC Isotope Geosciences Laboratory, British Geological Survey, Nottingham, UK

Abstract

Recent research has highlighted how Lake Baikal, Siberia, has responded to the direct and indirect effects of climate change (e.g., ice-cover duration), nutrient loading, and pollution, manifesting as changes in phytoplankton/zooplankton populations, community structure, and seasonal succession. Here, we combine and compare analyses of chlorophyll *a* (an estimate of total algal biomass), carotenoid pigments (biomarkers of algal groups), and lake water silicon isotope geochemistry ($\delta^{30}\text{Si}_{\text{DSi}}$) to differentiate spatial patterns in dissolved silicon (DSi) uptake at Lake Baikal. A total of 15 sites across the three basins (south, central, and north) of Lake Baikal were sampled in August 2013 along a depth gradient of 0–180 m. Strong, significant correlations were found between vertical profiles of photic zone DSi concentrations and $\delta^{30}\text{Si}_{\text{DSi}}$ compositions ($r = -0.81$, $p < 0.001$), although these are strongest in the central basin aphotic zone ($r = -0.98$, $p < 0.001$). Data refute the hypothesis of DSi uptake by picocyanobacteria. Algal biomass profiles and high surface $\delta^{30}\text{Si}_{\text{DSi}}$ compositions suggest greater productivity in the south basin and more oligotrophic conditions in the north basin. $\delta^{30}\text{Si}_{\text{DSi}}$ signatures are highest at depth (20 m) in central basin sites, indicating greater (10–40%) DSi utilization at deep chlorophyll maxima. DSi limitation occurs in the pelagic central basin, probably reflecting a high diatom biomass bloom event (*Aulacoseira baicalensis*). Meanwhile in the more hydrologically restricted, shallow Maloe More region (central basin), both high $\delta^{30}\text{Si}_{\text{DSi}}$ compositions and picocyanobacteria (zeaxanthin) concentrations, respectively point to the legacy of an “*Aulacoseira* bloom year” and continuous nutrient supply in summer months (e.g., localized eutrophication).

World-wide, climate warming is impacting freshwater ecosystems (e.g., O'Reilly et al. 2015) and, in many cases, its effects are superimposed upon anthropogenic catchment alteration, nutrient loading, and pollution (Jeppesen et al. 2011; Moss et al. 2011; Izmet'eva et al. 2016). Lake Baikal, the world's deepest and most voluminous lake (containing up to 20% of the world's unfrozen freshwater; Sherstyankin et al. 2006) is no exception. Over the past 60 yrs, surface-

water temperatures of Lake Baikal have increased up to 2.4°C (Hampton et al. 2008; Shimaraev and Domysheva 2013), resulting in earlier lake ice-off dates and later ice-on dates, particularly in the southern basin (Todd and Mackay 2003; Hampton et al. 2008). Ice formation and retreat, plays an essential role in the thermal regime of Lake Baikal, promoting water column mixing and upper water column nutrient renewal in the spring, after ice-off. As such, late 20th Century climate change has altered the water column thermal structure, which in turn has altered the spatial patterns of phytoplankton biomass (Fietz et al. 2007) and food web structure (Hampton et al. 2008).

Eutrophication has also been noted in the coastal and shallow bay regions of Lake Baikal (Kobanova et al. 2016), resulting in increases in cryptophyte blooms, toxin-forming cyanobacteria blooms and thick mats of the benthic,

*Correspondence: virginia.panizzo@nottingham.ac.uk

Additional Supporting Information may be found in the online version of this article.

This is an open access article under the terms of the Creative Commons Attribution License, which permits use, distribution and reproduction in any medium, provided the original work is properly cited.

filamentous chlorophyte *Spirogyra* spp., and the non-native macrophyte *Elodea canadensis* (Kravtsova et al. 2014; Kobanova et al. 2016; Timoshkin et al. 2016). The combined effects of climate and eutrophication on food web structures across pelagic and shallow regions need to be addressed in Lake Baikal (O'Donnell et al. 2017). This is of particular importance, as bottom up controls (e.g., nutrient availability and temperature) on phytoplankton productivity, are not well understood.

The limnological characteristics of Lake Baikal and importance of silicon stable isotope geochemistry

Assessment of the internal fluxes of nutrients in Lake Baikal are an important prerequisite for evaluating the consequences of climate and anthropogenic changes (Müller et al. 2005). Spring pelagic upwelling lasts c. 35 days and between 20% and 60% of the lake area mixes vertically (Shimaraev et al. 2012). Complete deep-water surface renewal is within the range of every 8–19 yrs (Weiss et al. 1991; Hohmann et al. 1997; Peeters et al. 1997; Müller et al. 2005). Instead, the top 200–300 m of the Lake Baikal water column convectively mixes twice each year (Shimaraev et al. 1994).

Dissolved silicon (DSi) is a vital nutrient for biomineralization in Lake Baikal (particularly in “*Aulacoseira* bloom years”: “Phytoplankton succession at Lake Baikal and seasonal nutrient uptake” section) and estimations of silicate residence time are between 100 yr and 170 yr (Falkner et al. 1997; Shimaraev and Domysheva 2004). Long-term export of DSi to Lake Baikal sediments (modelled to be 20–24%) is greater in the south than the north basin (Panizzo et al. 2017) due to better below-ice conditions (e.g., less snow cover and greater transparency), longer-ice free seasons, and subsequent enhanced diatom productivity. Surface-water DSi concentrations in Lake Baikal are predominantly derived from upwelling (630 mmol yr⁻¹), rather than riverine inputs (312 mmol yr⁻¹), and net sedimentation is estimated at c. 1170 mmol m⁻² yr⁻¹ (Müller et al. 2005).

Silicon isotope geochemistry provides the unique opportunity to model DSi uptake across the lake, identify productivity “hotspots” and explore drivers of these trends. Silicon (Si), the second most abundant element in the earth's crust (Epstein 1999), plays a key role in global biogeochemical cycling. The dissolved phase or DSi, also known as orthosilicic acid (Si(OH)₄), is an important nutrient in aquatic systems and has such been found to have an intimate relationship with the carbon cycle (via the oceanic biogeochemical pump; Pondaven et al. 2000). Si has three stable isotopes (²⁸Si, ²⁹Si, and ³⁰Si), which are reported via the delta notation $\delta^{30}\text{Si}$ as the ratio between ³⁰Si/²⁸Si (or previously $\delta^{29}\text{Si}$ as the ratio between ²⁹Si/²⁸Si) compared to the same ratio in the standard reference material NBS 28. These three isotopes of Si permit the method to be used as a proxy for constraining the silicon cycle due to the significant fractionations that occur during different processes. For example,

silicon isotope ratios of DSi in waters (referred to as $\delta^{30}\text{Si}_{\text{DSi}}$ hereafter) can be used as a tracer of multiple processes including weathering congruency (Fontorbe et al. 2013; Hughes et al. 2013; Frings et al. 2015), biological uptake and land-use changes (Delvaux et al. 2013), and anthropogenic catchment impacts (Hughes et al. 2012). In lakes, $\delta^{30}\text{Si}_{\text{DSi}}$ traces DSi nutrient utilization by siliceous organisms (Alleman et al. 2005; Opfergelt et al. 2011; Panizzo et al. 2016, 2017). Lake Baikal summer $\delta^{30}\text{Si}_{\text{DSi}}$ water column compositions have been demonstrated to provide a proxy for spring diatom utilization (Panizzo et al. 2016, 2017). For example, diatoms discriminate against the heavier ³⁰Si isotope during DSi uptake with the lighter ²⁸Si isotope incorporated via biomineralization, leading to the residual DSi pool becoming enriched in ³⁰Si. Panizzo et al. (2016) identified the progressive isotopic enrichment of diatoms ($\delta^{30}\text{Si}_{\text{diatom}}$) during spring bloom development, so that summer compositions (when stratification ensues) reflect the legacy of this spring diatom bloom.

Here, we explore similarities and differences in biogeochemical cycling across the upper water column (0–180 m) of Lake Baikal. We present the first lake system comparisons of phytoplankton biomass [chlorophyll *a* (Chl *a*) concentrations], phytoplankton composition (algal chlorophyll and carotenoid pigments), and seasonal DSi utilization ($\delta^{30}\text{Si}_{\text{DSi}}$). Combined, these proxies provide the opportunity to test the hypothesis that picocyanobacteria do not substantially alter the DSi pool, when their populations dominate the summer phytoplankton (“Phytoplankton succession at Lake Baikal and seasonal nutrient uptake” and “Examining main drivers behind DSi uptake at Lake Baikal” sections). Our second objective is to better understand how internal cycling of DSi varies spatially across Lake Baikal (both in pelagic and more shallow regions) (“Spatial patterns of DSi utilization at Lake Baikal” section). Finally, the novel approach of silicon isotope geochemistry will be used to quantify seasonal DSi utilization at depth and explore episodes of localized nutrient exhaustion, as a response to both these natural and anthropogenic pressures (“Quantifying sub-surface DSi utilization at central basin sites in Lake Baikal” section).

Phytoplankton succession at Lake Baikal and seasonal nutrient uptake

Annually, the first phytoplankton (diatom) blooms in Lake Baikal occur in spring under ice, and thus lake-ice duration and transparency are crucial to their development (Jewson et al. 2009; Moore et al. 2009). Seasonal succession of phytoplankton blooms is linked to the timing of ice-off (end of May–June) when a rapid period of diatom cell-division occurs, as a result of the turbulent mixing of the water column to a depth of c. 100 m (Popovskaya 2000; Fietz et al. 2005a). In autumn (after October), as summer stratification breaks down, a second peak in diatoms (including *Cyclotella minuta* species) occurs due to turbulent mixing and cell

resuspension from the deeper waters. This bloom is smaller than in the spring as convective mixing is deeper (reducing light availability) and grazing pressures greater (Popovskaya 2000).

During the spring bloom period (May–June), diatoms can comprise 50–90% of phytoplankton biomass in the lake and are strongly correlated with DSi availability (but not nitrogen [N] and phosphorus [P]) (Popovskaya et al. 2015). This relationship between DSi and diatoms is particularly evident during “*Aulacoseira baicalensis* (previously termed *Melosira*) bloom” years and hereafter referred to as “*Aulacoseira* bloom years,” which occur on 3–4 yr cycles. “*Aulacoseira* bloom years” are periods of high diatom production, commencing under ice, when algal biomass is up to 10 times higher than non-“*Aulacoseira* bloom years” (Bondarenko and Evstafev 2006; Jewson et al. 2010). Definitive explanations for *Aulacoseira baicalensis* blooms have previously been proposed to be either meteorologically (Shimaraev 1971) or internally driven by lake processes (e.g., lake water temperatures, Kozhova 1955; and/or light and nutrient availability, Kozhova 1960). More recently, ice transparency is perceived to be a critical driver promoting these blooms in the spring, as a result of preceding autumnal meteorological conditions which favor clear ice formation (Katz et al. 2015). Additionally, deeper convective spring mixing depths (up to 100 m) and therefore nutrient renewal, is thought to account for the competitive increase of this species in “*Aulacoseira* bloom years” (over other diatom taxa) due to its high DSi demand (Jewson et al. 2010). Over the last 50 yr, the timing of “*Aulacoseira* blooms” (within a year) has shifted later by up to 1.6 months, and this shift is thought to be linked to the delay in the timing of ice formation in the autumn (Katz et al. 2015).

Thermal stratification plays a key role in determining phytoplankton communities in Lake Baikal, via direct (e.g., buoyancy) and indirect (e.g., nutrient redistribution) mechanisms (Klausmeier and Litchman 2001; Diehl et al. 2002; Fietz et al. 2005a; Hampton et al. 2014). As water temperatures increase and the summer stratification develops, larger diatoms sink to depths of c. 200–300 m which initiates resting stage formation in *A. baicalensis* (Kozhova and Izmet'eva 1998). In contrast, smaller centric diatoms (e.g., *C. minuta*) can persist in the upper water column into summer (Popovskaya 2000), but phytoplankton become dominated by picocyanobacteria (*Synechocystis limnetica*) (up to 80% of primary production; Belykh et al. 2006), because the taxa are adapted to the warmer, low-nutrient, and higher irradiance conditions in the stratified water column (Fietz et al. 2005b; Hampton et al. 2008).

Recent experimental work has identified that N, P (Satoh et al. 2006) and, in certain instances, both (co-limitation; O'Donnell et al. 2017) are the strongest predictors of summer picocyanobacteria (measured as Chl *a*) in Lake Baikal. When non-siliceous picocyanobacteria dominate the

summer phytoplankton assemblages (60–100%), DSi limitation would not necessarily be expected (Nagata et al. 1994; Fietz et al. 2005b; O'Donnell et al. 2017). However, in Lake Baikal, it is probable that large spring diatom blooms (e.g., in “*Aulacoseira* bloom years” or as a response to regional eutrophication) have significant legacy impacts on summer nutrient availability and annual phytoplankton succession. For example, in other lakes, lower ambient spring DSi concentrations can restrict diatom biomass, leading to greater summer P availability and higher summer cyanobacterial biomass (Krivtsov et al. 2000). In combination with ongoing increases in nutrient loading and surface-water temperatures (Hampton et al. 2008; Hampton et al. 2014; Izmet'eva et al. 2016; Timoshkin et al. 2016), these pelagic successional processes may, in turn, have implications for the long-term bioavailability of nutrients (e.g., DSi) in Lake Baikal. Furthermore, evidence from oceanic environments indicates that growth of picoplankton cells can significantly deplete regional biogenic silica (BSi) stocks, pointing to the potential need to revise interpretations of particulate matter elemental ratios (e.g., Si : C) in these environments (Krause et al. 2017). Evidence from cultured marine phytoplankton further supports the substantial role of marine picocyanobacteria (*Synechococcus*) in the modification of silica cycling (Baines et al. 2012). Sigeo and Levado (2000) have equally identified sub-populations of freshwater cyanobacteria *Microcystis aeruginosa* in Rostherne Mere, UK, where cell surface Si concentrations were elevated compared to other sub-populations. The mechanisms attributable to this Si accumulation (whether internal or external to the cell), both in freshwater and marine-water picocyanobacteria, remain poorly constrained (Baines et al. 2012; Durkin et al. 2016), although some evidence proposes *Synechococcus* cells to act as a nucleating site for mineral formation (Schultze-Lam et al. 1992), which either contains Si or permits Si adsorption (Nelson et al. 1984). Although initial evidence of Si accumulation in picocyanobacteria cells has been documented in small freshwater lake systems (e.g., Sigeo and Levado 2000; Krivtsov et al. 2005), Lake Baikal's great size means that physical processes have much in common with marine environments, where nutrient cycling is substantially influenced by upwelling (as a function of lake water temperatures and stratification timing/duration; Fietz et al. 2005a). This study will therefore aim to examine the hypothesis of Si bioaccumulation by picocyanobacteria in Lake Baikal.

Materials

Site description and sampling

Lake Baikal is made up of three distinct basins (south, central, and north), separated by two underwater highs: the Academician Ridge in the north and the Selenga Shallows in the south (Fig. 1). Distinct limnological differences exist between the southern and northern basins due to a

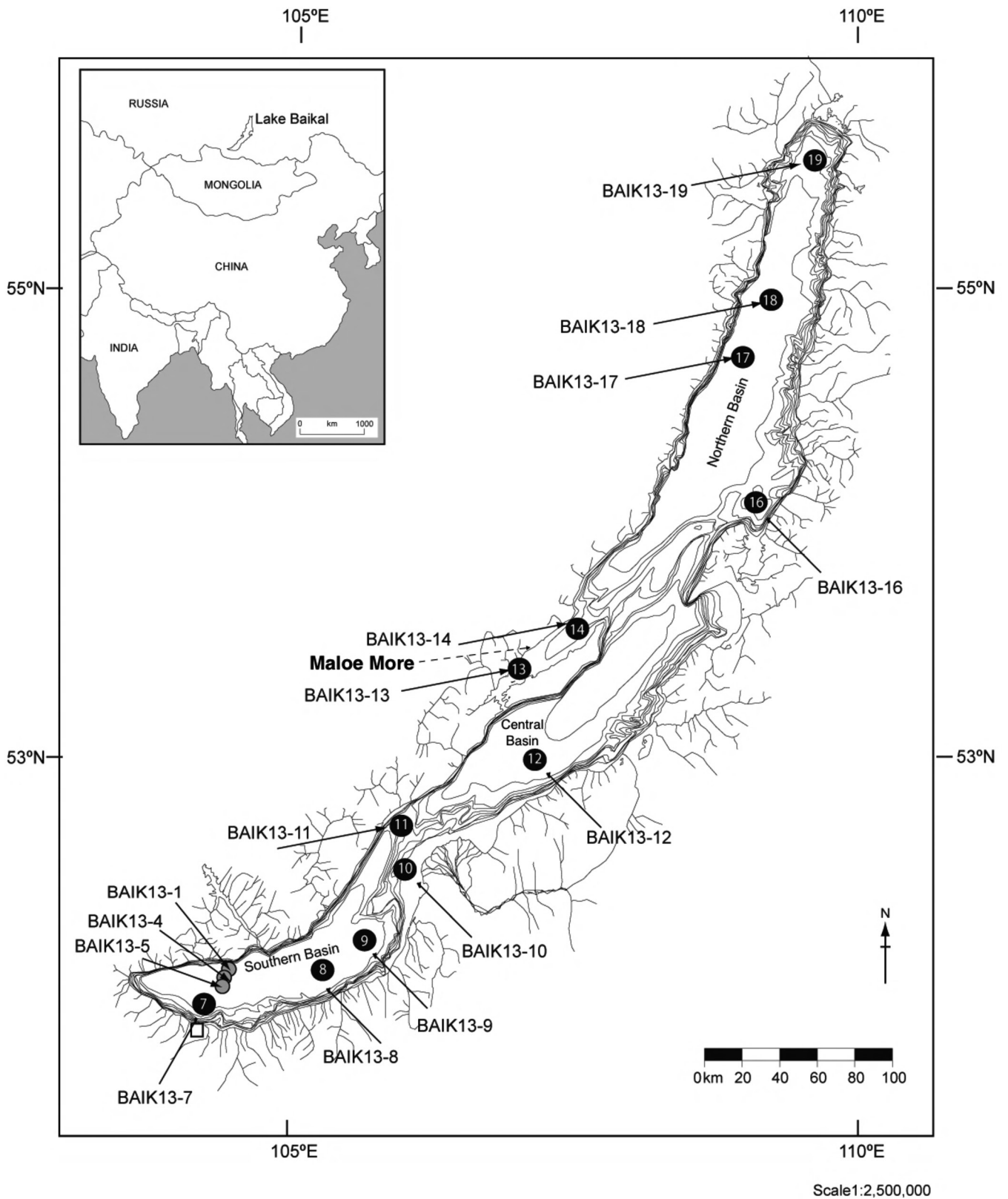


Fig. 1. Map of the Lake Baikal region with locations of all water profile data collection highlighted. Refer to Supporting Information Table S1 for all data corresponding to respective sites. All samples were collected in August 2013.

combination of factors including the large latitudinal and climatic range that they span, but also their geomorphologies and hydrological inputs. Water samples were collected in August 2013 from 15 sites across Lake Baikal (Fig. 1), after the period of turbulent spring mixing, and during summer lake stratification. Sampling was conducted between late July and mid-August 2013, over a 4-week period. Sampling conditions remained calm and stable throughout, although strong underwater currents were experienced when sampling at site BAIK13-5, which impeded completing deep-water profile sampling of light meter data (e.g. an absence of photic zone depth calculation; Supporting Information Table S1). We focus on the upper 180 m of the water column as this captures the zone of phytoplankton activity and depths where both spring and autumn convective mixing occurs, and significant surface-water temperature increases are being recorded (Hampton et al. 2014). Sites BAIK13-1 to BAIK13-11 constitute south basin sites, BAIK13-12 to BAIK13-14 are central basin (including the relatively shallow [c. 200 m] more hydrologically restricted Maloe More sites) and BAIK13-16 to BAIK13-19 are north basin sites (Fig. 1). Refer to Fig. 1 and Supporting Information Table S1 for exact locations.

A 2 L Van Dorn sampler was used to sample waters at depths of 1 m, 3 m, 5 m, 10 m, 20 m, 30 m, 100 m, and 180 m for analysis of algal pigments (however, the depth of 50 m was additionally sampled for sites BAIK13-1, 4, and 5 only; to match March 2013 sampling resolutions) and depths of 1 m, 20 m, 50 m, 100 m, and 180 m for DSi concentrations and $\delta^{30}\text{Si}_{\text{DSi}}$ analysis. These were accompanied by measurements of light intensity (photosynthetically active radiation between 400 nm and 700 nm) every 1 m to a maximum depth of 70 m using a LI-COR light meter. Light attenuation coefficients ($K_d \text{ m}^{-1}$) were calculated at each water-sampling site from the irradiance vs. depth relationship of LI-COR data, which was log-linearly constrained (Supporting Information Table S1). Continuous Chl *a* measurements were also collected at each site, to a depth of 180 m, using a YSI XO2 sonde (in $\mu\text{g L}^{-1}$ later converted to nmol L^{-1}). These data were also validated via discreet, in situ Chl *a* measurements via high-performance liquid chromatography (HPLC) and spectrophotometry techniques and were selected to report due to their continuous and high-resolution water profile sampling. Deep chlorophyll maxima (DCM) thickness was determined from values greater than 90% of the total chlorophyll average within the water profile. A depth correction was applied to the YSI sonde dataset to consider drift while sampling down the water column, which generally only affected samples below 50 m. Photic zone depths for each site were defined as the depth at which < 1% of the surface light is measured (as per Saros et al. 2005).

Phytoplankton pigment analyses

Compositional biomass of phytoplankton groups was estimated using the algal carotenoids fucoxanthin (from

diatoms and chrysophytes [the former are much more abundant in Lake Baikal] and zeaxanthin (a general biomarker for cyanobacteria, of which picocyanobacteria are most abundant in Lake Baikal) from water samples collected as above (0–180 m). Water samples were filtered through a Whatman GF/F (0.45 μm pore size) filter, which was stored in the dark and frozen until analysis at the University of Nottingham. Filtered substrates were extracted in an acetone, methanol, and water mixture (80 : 15 : 5), filtered using a 0.22 μm polytetrafluoroethylene (PTFE) filter, dried under nitrogen gas and re-dissolved before injection into the HPLC unit (Agilent 1200 series). Separation methods used are detailed in McGowan et al. (2012). Pigments were identified and quantified from the chromatograms by comparing retention times and spectral characteristics with calibration standards (DHI Denmark).

Silicon isotope preparation and analysis

Samples for $\delta^{30}\text{Si}_{\text{DSi}}$ analyses were filtered through 0.4 μm Whatman polycarbonate filters before storage in acid washed low density polyethylene (LDPE) bottles and acidification with Romil UPA HCl (10 M) to a pH close to 2. Aliquots of Si samples were taken on return to the lab at the British Geological Survey for inductively coupled plasma-mass spectrometry (ICP-MS) analyses (Agilent Technologies 7500). Samples were purified through cation column chemistry as per Georg et al. (2006) in order to obtain an optimal silicon concentration of between 3 ppm and 10 ppm. DSi concentrations are referred to as ppm as this is how they were reported after ICP-MS. However, they have been converted to μM for comparison with other data sets and also to permit comparisons with pigment data.

Samples were analyzed in wet-plasma mode using the high mass-resolution capability of a Thermo Scientific Neptune Plus multi collector inductively coupled plasma mass spectrometer at the British Geological Survey. Sample preparation and instrument details are summarized in Panizzo et al. (2016, 2017), along with details on procedural blank methods, calculations, and sample analytical errors. Procedural blank amounts ranged from 5 ng to 15 ng. The blank isotope composition ($\delta^{30}\text{Si}$) most different to the average sample composition differed by only c. 0.4‰ and this was within uncertainty of the blank isotopic compositional measurement. Ignoring the uncertainty, the amount and composition of this blank would have contributed a shift of < 0.015‰ in the sample $\delta^{30}\text{Si}$ compositions, well within the method uncertainty of 0.15‰. As such, contributions to sample compositions from procedural blank are considered to be negligible and no blank correction has been applied. All uncertainties are reported at 2σ absolute, and incorporate an excess variance derived from the whole data-set Diatomite validation material. The long-term variance for Diatomite = $+1.24 \pm 0.18\%$ (2 SD, $n = 244$) (consensus value

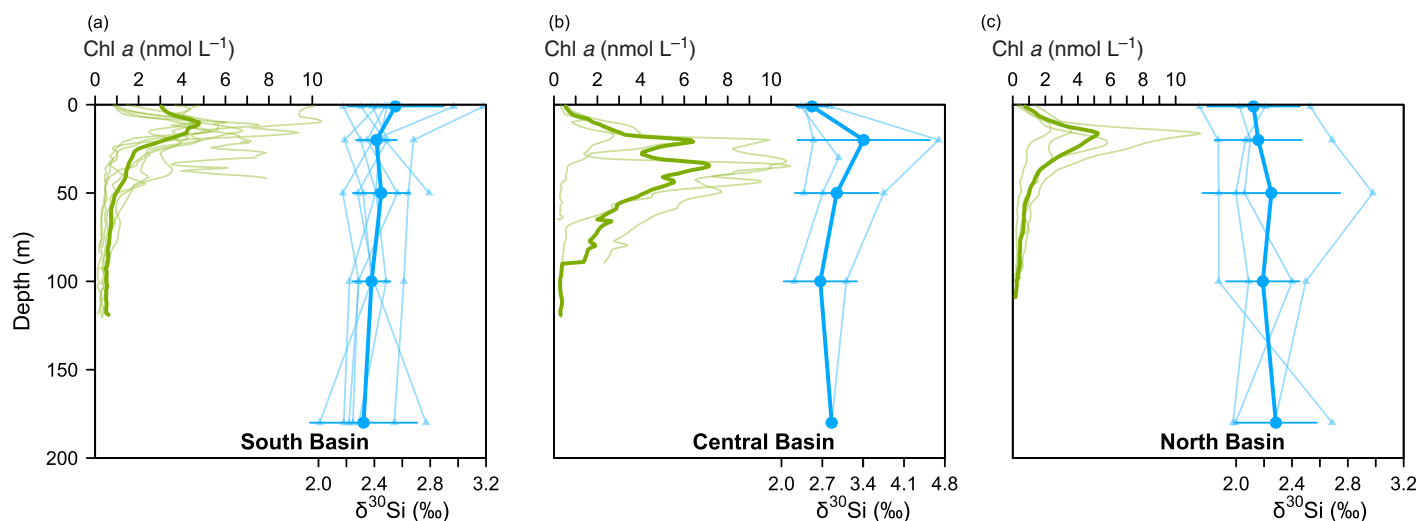


Fig. 2. Composite water column profiles of Chl *a* (nmol L⁻¹; green bold) and $\delta^{30}\text{Si}_{\text{DSi}}$ (‰; blue bold) as a function of depth. Data are presented for the south (a), central (b), and north (c) Lake Baikal basins. Individual site data are presented (as shadow lines) and the derived composite (with respective 1 SD for $\delta^{30}\text{Si}_{\text{DSi}}$ data only) is superimposed. Please refer to Fig. 3 for individual site plots. [Color figure can be viewed at wileyonlinelibrary.com]

of $+1.26 \pm 0.2\text{‰}$, 2 SD; Reynolds et al. 2007) and the in-house standard RMR4 = $+0.88 \pm 0.20\text{‰}$ (2 SD, $n = 42$).

Data analysis

For each sample, fucoxanthin pigment concentrations were normalized to DSi concentrations. This provides a means to assess whether diatom utilization is accounting for Si isotopic fractionation in the water column: assumed, by general interpretation, that this will account for the higher isotopic compositions and lower DSi concentrations in waters (cf. Zhang et al. 2015). Fucoxanthin concentrations (nmol L⁻¹) were converted to $\mu\text{g L}^{-1}$ applying the molecular weight of fucoxanthin (658.92) and normalizing to DSi (μM). Hereafter, the ratio will be referred to fucoxanthin/DSi ($\mu\text{g}/\mu\text{M}$). This calculation was also made for zeaxanthin/DSi ($\mu\text{g}/\mu\text{M}$) in order to hypothesis test the absence of picocyanobacteria (molecular weight of 568.88) DSi uptake.

Data presented here also provides the opportunity to use silicon stable isotope geochemistry to quantify diatom utilization of DSi at DCM in Lake Baikal. This work builds on the earlier estimations of Panizzo et al. (2017), conducted on surface waters alone. Full descriptions on the principles and approaches used to model utilization through $\delta^{30}\text{Si}_{\text{DSi}}$ compositional data are presented in Panizzo et al. (2017), with full justification for the model (open/steady state vs. closed/Rayleigh) and diatom uptake fractionation factors applied.

Results

Spatial patterns in Chl *a*, fucoxanthin, and zeaxanthin concentration

Chl *a* concentrations were higher in south basin surface waters (0.94–9.48 nmol L⁻¹) than the central (0.46–0.53

nmol L⁻¹) and north basin sites (0.34–1.40 nmol L⁻¹) (Fig. 2a–c), highlighting shallower algal production in the south basin, while greater deeper water algal production was seen in the central and north basins (Fig. 2b,c). Composite summaries of Chl *a* concentrations demonstrate the greater variability at depth for the central basin (Fig. 2b), where a deeper, more defined peak at 20–50 m water depth is seen. This deeper Chl *a* peak in the central basin (Fig. 2b), reached values much greater than those from the south basin (e.g., ranges between 1.97–12.00 nmol L⁻¹ and 0.17–8.24 nmol L⁻¹ at 20 m and 50 m depth, respectively; Fig. 3, Supporting Information Table S1). Similarly, more-defined sub-surface peaks (between 10 m and 20 m; Supporting Information Table S1) of Chl *a* are also identified in the north basin (Fig. 3), compared with south basin sites.

Composite profiles of zeaxanthin concentrations showed highest values in south basin surface waters, followed by the north basin with general trends showing a decrease in concentrations with depth (Fig. 4a,c). However, zeaxanthin concentrations showed a peak at depth (20 m) for central basin sites (Fig. 4b). Similarly, fucoxanthin concentrations in the south basin surface waters were higher compared to the central and north basin sites (concentrations range between c. 0.03 nmol L⁻¹ and 0.37 nmol L⁻¹; Fig. 4b,c), while they were greater at depth for the pelagic central, Maloe More embayment and north basins (20 m; Fig. 4b,c), particularly at sites BAIK13-12 and BAIK13-14 (depths of 30 m and 100 m, respectively; Fig. 5).

Water profiles of DSi concentrations and $\delta^{30}\text{Si}_{\text{DSi}}$ compositions in Lake Baikal

Typical values of DSi concentrations for surface-water samples were significantly (although weakly so) greater

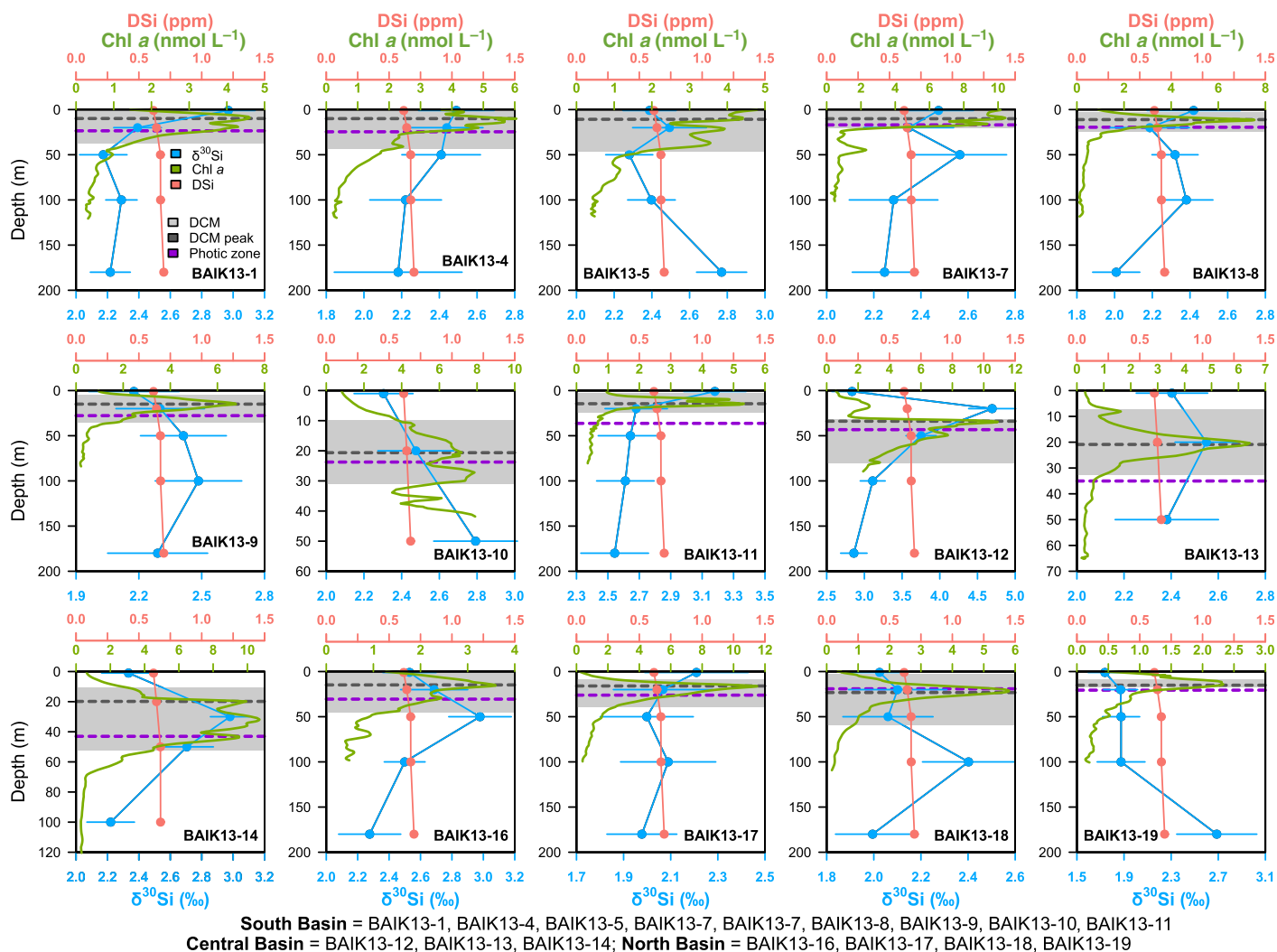


Fig. 3. Water column profile data for all of the Lake Baikal sites ($n = 15$). Data include Chl a (nmol L^{-1}) in green, DSi concentrations (ppm) in orange, and $\delta^{30}\text{Si}_{\text{DSi}}$ (‰) in blue (latter with respective analytical uncertainties). Superimposed upon each plot are the photic zone depth (purple dashed line) and peak DCM depth (dark gray dashed line) in meters (both calculations are defined in “Site description and sampling” section). Overall DCM depth (m) for each site is also provided as a shaded gray area. Station label names are given and their corresponding basin location provided (e.g., south basin, central basin, and Maloe More or the north basin). [Color figure can be viewed at wileyonlinelibrary.com]

($p = 0.038$) in the north basin (0.49–0.93 ppm) than the south and central basins (0.13–0.70 ppm) ($n = 71$; Supporting Information Table S1). Water column profiles showed a general increase in DSi concentrations below the surface (Fig. 3), apart from at sites BAIK13-7 and BAIK13-12 where there was considerable variability (Supporting Information Table S1). However, vertical changes in DSi concentrations from 0 m to 180 m were less than those observed in deep waters below 500 m (Panizzo et al. 2017). We attributed a cutoff sampling depth of 20 m for the photic zones, for the purpose of conducting correlation significance testing. This is to do with the sampling resolution of silicon concentration and isotope analyses (0 m, 20 m, 50 m, 100 m, and 180 m). In particular, lake-wide photic zone measurements from August 2013

(16.9–43.2 m) were above the 50 m sampling interval for $\delta^{30}\text{Si}_{\text{DSi}}$ (“Site description and sampling” section) and therefore the cutoff sampling depth of 20 m (Table 1) was applied in order to match pigment data with the sampling intervals adopted for silicon isotope analyses (“Site description and sampling” section).

$\delta^{30}\text{Si}_{\text{DSi}}$ display an inverse relationship with DSi concentrations down the water column ($r = -0.81$, $p < 0.001$; Table 1). In the south basin, $\delta^{30}\text{Si}_{\text{DSi}}$ signatures were higher in surface waters (+2.18 to +3.18‰; coincident with the high surface Chl a , zeaxanthin and fucoxanthin concentrations) except at sites BAIK13-5, BAIK13-9, and BAIK13-10 (although data fall within analytical uncertainty [AU]; Supporting Information Table S1)(Figs. 3, 5). The opposite was seen in

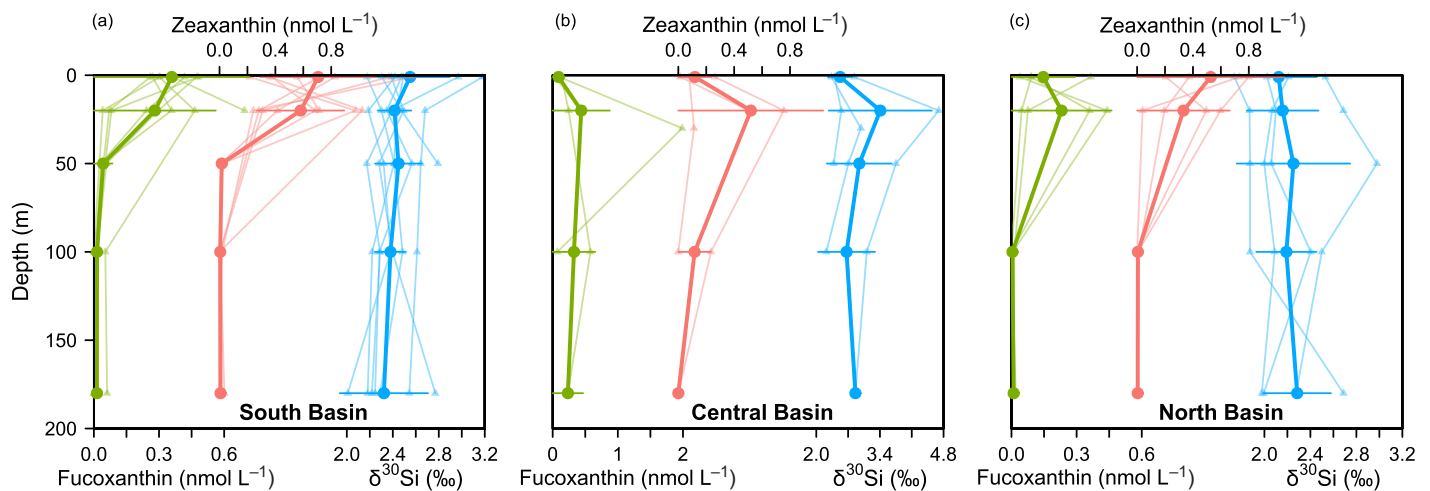


Fig. 4. Composite water column profiles of fucoxanthin concentrations (nmol L^{-1} ; green bold), zeaxanthin concentrations (nmol L^{-1} ; orange bold), and $\delta^{30}\text{Si}_{\text{DSi}}$ (‰; blue bold) as a function of depth. Data are presented for the south (a), central (b), and north (c) Lake Baikal basins. Individual site data are presented (as shadow lines) and the derived composite (with respective 1 SD) is superimposed in bold. Please refer to Fig. 5 for individual site plots. [Color figure can be viewed at wileyonlinelibrary.com]

the north basin, where surface-water $\delta^{30}\text{Si}_{\text{DSi}}$ compositions (+1.74 to +2.53‰) were lower than deeper water samples (Fig. 2c; apart from site BAIK13–17 [although within AU; Supporting Information Table S1]; Figs. 3, 5). This trend in the north basin extended to the central basin (BAIK13-12, BAIK13-13, and BAIK13-14) and was particularly noted at the pelagic site BAIK13-12 where values at 20 m were considerably higher ($+4.69 \pm 0.31\%$) than the upper waters (Figs. 2b, 3). Here, $\delta^{30}\text{Si}_{\text{DSi}}$ signatures have distinctive profiles, with subsurface maxima of Chl *a*, fucoxanthin, and zeaxanthin, associated with among the highest $\delta^{30}\text{Si}_{\text{DSi}}$ isotopic compositions across the lake (between +2.55 and +4.69‰) (Fig. 2b).

Basin wide patterns in $\delta^{30}\text{Si}_{\text{DSi}}$

Strong leverage is identified from values at BAIK13-12 when correlating $\delta^{30}\text{Si}_{\text{DSi}}$ compositions and DSi concentrations across Lake Baikal (higher $\delta^{30}\text{Si}_{\text{DSi}}$ compositions and lower DSi concentrations) (Table 1). The removal of this outlier still resulted in a significant, negative relationship ($r = -0.76$, $p < 0.001$; Fig. 6). Negative correlations for all sites, between lake water $\delta^{30}\text{Si}_{\text{DSi}}$ signatures and DSi concentrations were stronger for the photic zone (< 20 m) ($r = -0.86$, $p < 0.001$) than for waters below the photic zone (> 20 m) ($r = -0.47$, $p < 0.001$) (Fig. 4a,c). These relationships were strongest in the south and north basin photic zone ($r = -0.84$ and $r = -0.93$, respectively, $p < 0.001$) and not significant in the central basin (Table 1). Aphotic zone negative correlations between $\delta^{30}\text{Si}_{\text{DSi}}$ and DSi were highly significant in central basin sites ($r = -0.98$, $p < 0.001$) but weaker in the south basin ($r = -0.69$, $p < 0.001$; Table 1).

There was an absence of significant correlations between $\delta^{30}\text{Si}_{\text{DSi}}$ and fucoxanthin concentrations and $\delta^{30}\text{Si}_{\text{DSi}}$ and zeaxanthin concentrations for all lake wide and basin wide,

photic zone data (data not shown). However, fucoxanthin/DSi ratios in the photic zone across all lakes sites had a strong, significant and positive relationship ($r = +0.88$, $p < 0.001$) with $\delta^{30}\text{Si}_{\text{DSi}}$ (Fig. 7). Similarly, correlations for photic zone zeaxanthin/DSi ratios and $\delta^{30}\text{Si}_{\text{DSi}}$ were also positive and significant ($r = +0.83$, $p < 0.001$). Indeed, the strongest, significant correlation coefficients were derived for all central basin photic zone data between $\delta^{30}\text{Si}_{\text{DSi}}$ and fucoxanthin/DSi ratios ($r = +0.99$, $p < 0.001$) and $\delta^{30}\text{Si}_{\text{DSi}}$ and zeaxanthin/DSi ratios ($r = +0.97$, $p < 0.001$). Interestingly, an absence of strong, significant correlations between $\delta^{30}\text{Si}_{\text{DSi}}$ vs. fucoxanthin/DSi and zeaxanthin/DSi ratios existed for south and north basin photic zone data and only moderate significant correlations for lake-wide aphotic zone data ($r = +0.77$ and $r = +0.39$, $p < 0.001$, respectively; Table 1).

Discussion

Examining main drivers behind DSi uptake at Lake Baikal

Strong, negative correlations exist between DSi and $\delta^{30}\text{Si}_{\text{DSi}}$ signatures, most notable in the photic zone of the south and north basins ($r = -0.84$ and $r = -0.93$, respectively; Table 1) and also in the aphotic zone in the central basin ($r = -0.98$; Table 1). This relationship reflects DSi uptake by diatoms (lower DSi surface concentrations) due to discrimination against the ^{30}Si isotope in the spring months (Panizzo et al. 2016). Other studies have also demonstrated that diatom biomass correlates with DSi availability (rather than N and P) (data from 2001 to 2003; Fietz et al. 2005b). However, we here further test the hypothesis that picocyanobacteria are significantly influencing DSi uptake at Lake Baikal (cf. Baines et al. 2012; Krause et al. 2017).

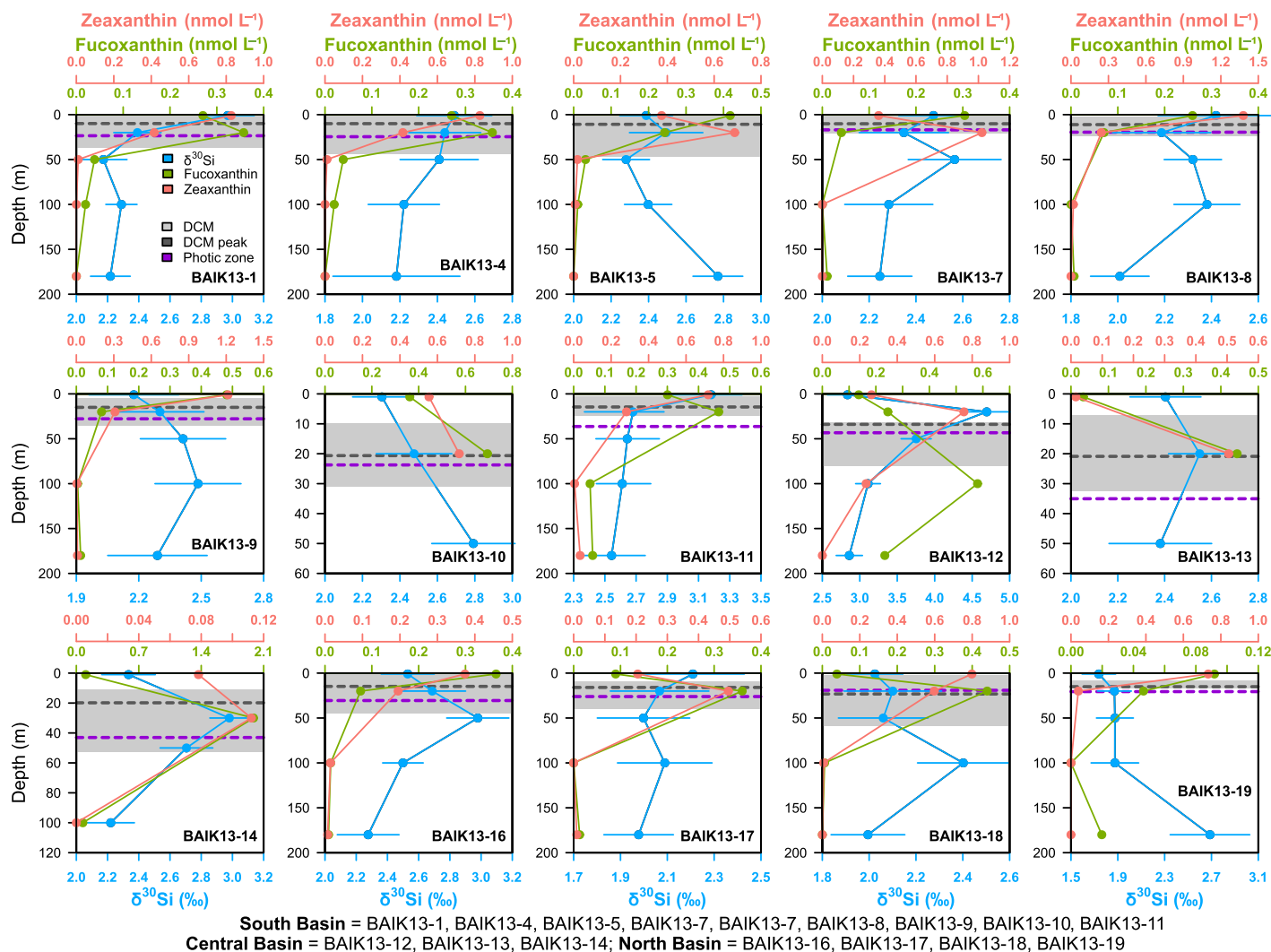


Fig. 5. Water column profile data for all of the Lake Baikal sites ($n = 15$). Data include fucoxanthin concentrations (nmol L^{-1}) in green, zeaxanthin concentrations (nmol L^{-1}) in orange, and $\delta^{30}\text{Si}_{\text{DSi}}$ (‰) in blue (with respective analytical uncertainties). Superimposed upon each plot is the photic zone depth (m) for each site (purple dashed line). Note that pigment analyses were not possible for the depth 50 m at sites BAIK13-10 and BAIK13-13 due to shallower water depths. Peak DCM depth (dark gray dashed line) in meters is also shown and overall DCM depth (m) for each site is provided as a gray shaded area. Station label names are given and their corresponding basin location provided (e.g., south basin, central basin, and Maloe More or the north basin). [Color figure can be viewed at wileyonlinelibrary.com]

A strong significant, positive correlation exists between lake-wide, photic zone $\delta^{30}\text{Si}_{\text{DSi}}$ and fucoxanthin/DSi ratios ($r = +0.88$; Fig. 7), which is greater than between $\delta^{30}\text{Si}_{\text{DSi}}$ and zeaxanthin/DSi ratios ($r = +0.83$; Table 1). The lake-wide correlation between $\delta^{30}\text{Si}_{\text{DSi}}$ and zeaxanthin/DSi ratios is driven by the central basin sites (BAIK13-12,13,14; $r = +0.97$; Table 1), with no significant correlations ($r = +0.11$) between combined south and north basin data. Similarly, a weak positive although significant, correlation is identified for lake-wide aphotic zone fucoxanthin ($r = +0.77$) and zeaxanthin ($r = +0.69$) data, although no such significant correlations between these parameters are seen for independent basins (Table 1). Although central basin aphotic correlations are not

significant, they are strong (Table 1), and reasons attributable to these positive relationships at these sites will be explored below.

Annual phytoplankton succession at Lake Baikal is well documented (“Phytoplankton succession at Lake Baikal and seasonal nutrient uptake” section), with diatoms (fucoxanthin) dominating under-ice and spring phytoplankton assemblages (50–90%; Popovskaya et al. 2015), followed by a summer assemblage dominated by picocyanobacteria (zeaxanthin). Therefore, we argue that the absence of correlations between south and north basin photic zone $\delta^{30}\text{Si}_{\text{DSi}}$ and fucoxanthin/DSi ratios is caused by sampling during the summer months when phytoplankton succession means

Table 1. Lake-wide and basin-wide correlation coefficients and significance testing results for $\delta^{30}\text{Si}_{\text{DSi}}$ vs. DSi concentrations, $\delta^{30}\text{Si}_{\text{DSi}}$ vs. fucoxanthin/DSi, $\delta^{30}\text{Si}_{\text{DSi}}$ vs. zeaxanthin/DSi. Data presented for the photic and aphotic zones as defined in “Water profiles of DSi concentrations and $\delta^{30}\text{Si}_{\text{DSi}}$ compositions in Lake Baikal” section, as well as all sampling depths, presented. Correlations, which are significant, are shaded in gray.

	Photic zone					
	$\delta^{30}\text{Si}_{\text{DSi}}$ vs. DSi		$\delta^{30}\text{Si}_{\text{DSi}}$ vs. fucoxanthin/DSi		$\delta^{30}\text{Si}_{\text{DSi}}$ vs. zeaxanthin/DSi	
	<i>r</i>	<i>p</i> value	<i>r</i>	<i>p</i> value	<i>r</i>	<i>p</i> value
Lake-wide (<i>n</i> = 30)	-0.86	<0.001	+0.88	<0.001	+0.83	<0.001
South (<i>n</i> = 16)	-0.84	<0.001	+0.39	0.144	+0.38	0.166
Central (<i>n</i> = 6)	-0.78	0.067	+0.99	<0.001	+0.97	<0.001
North (<i>n</i> = 8)	-0.93	<0.001	+0.17	0.277	-0.49	0.937
	Aphotic zone					
	$\delta^{30}\text{Si}_{\text{DSi}}$ vs. DSi		$\delta^{30}\text{Si}_{\text{DSi}}$ vs. fucoxanthin/DSi		$\delta^{30}\text{Si}_{\text{DSi}}$ vs. zeaxanthin/DSi	
	<i>r</i>	<i>p</i> value	<i>r</i>	<i>p</i> value	<i>r</i>	<i>p</i> value
Lake-wide (<i>n</i> = 41)	-0.47	<0.001	+0.77	<0.001	+0.69	<0.001
South (<i>n</i> = 22)	-0.69	<0.001	+0.27	0.293	+0.27	0.301
Central (<i>n</i> = 7)	-0.98	<0.001	+0.85	0.149	+0.71	0.294
North (<i>n</i> = 12)	-0.69	0.009	+0.73	0.024	+0.34	0.372
	All sampling depths					
	$\delta^{30}\text{Si}_{\text{DSi}}$ vs. DSi		$\delta^{30}\text{Si}_{\text{DSi}}$ vs. fucoxanthin/DSi		$\delta^{30}\text{Si}_{\text{DSi}}$ vs. zeaxanthin/DSi	
	<i>r</i>	<i>p</i> value	<i>r</i>	<i>p</i> value	<i>r</i>	<i>p</i> value
All depths (<i>n</i> = 71)	-0.81	<0.001	+0.82	<0.001	+0.74	<0.001

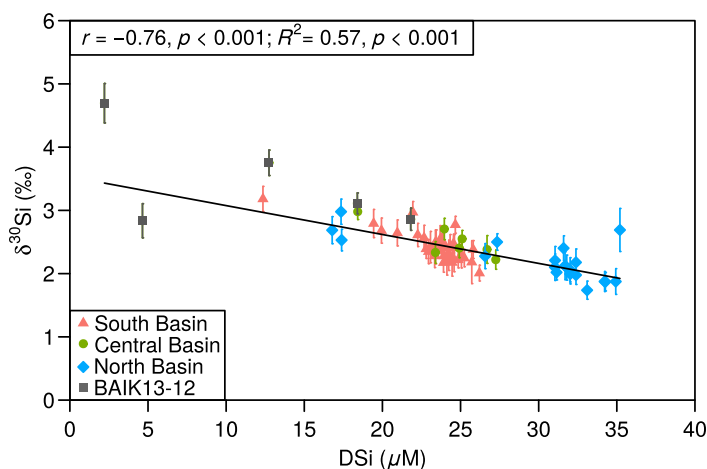


Fig. 6. DSi concentrations (μM) vs. $\delta^{30}\text{Si}_{\text{DSi}}$ (‰) for all water profile sample depths ($n = 71$) from each of the Lake Baikal basins, displayed with respective $\delta^{30}\text{Si}_{\text{DSi}}$ analytical uncertainties (2σ ; as cited in Supporting Information Table S1). A regression trend line is shown and significant correlation coefficients are also provided, although site BAIK13_12 data (gray squares) are not included. South (orange triangles), central (green circles), and north (blue diamonds) basin sites are all differentiated. [Color figure can be viewed at wileyonlinelibrary.com]

picocyanobacteria more abundant. Furthermore, we argue that the absence of correlations between south and north basin photic zone $\delta^{30}\text{Si}_{\text{DSi}}$ and zeaxanthin/DSi ratios,

supports our hypothesis that DSi uptake is not driven by picocyanobacteria (zeaxanthin) uptake.

We attribute the significant correlation between $\delta^{30}\text{Si}_{\text{DSi}}$ and zeaxanthin/DSi ratios at central basin and Maloe More sites (Table 1), to sampling in August when phytoplankton biomass was dominated by picocyanobacteria (zeaxanthin) (Fig. 4a,c). It is likely that this strong relationship is driven by pelagic site BAIK13-12 (Fig. 1), which shows a unique profile. Here, peak fucoxanthin concentrations (0.58 nmol L^{-1}) occur much deeper (100 m depth), while peak zeaxanthin concentrations (0.76 nmol L^{-1}) coincide with the highest $\delta^{30}\text{Si}_{\text{DSi}}$ signatures in the profile ($+4.69\text{‰}$ at 20 m; Fig. 5). As the fucoxanthin peak occurs below both the photic zone (43 m water depth) and the DCM (20 m; Fig. 5), we infer that it is recording a large sinking diatom bloom rather than in situ production. Therefore, the high $\delta^{30}\text{Si}_{\text{DSi}}$ values in the upper 20 m of the water column (Fig. 2b) record the waters enriched in ^{30}Si following spring diatom production before sinking of the valves commenced (supported by the strong, positive correlation between $\delta^{30}\text{Si}_{\text{DSi}}$ and fucoxanthin/DSi data: $r = +0.99$, $p < 0.001$; Table 1). Thus, sampling during the summer months (when picocyanobacteria are dominant: $r = +0.97$, $p < 0.001$) records the legacy effects of earlier diatom blooms, which initiate in the spring. Reasons accounting for the unique relationships between pigment and silicon

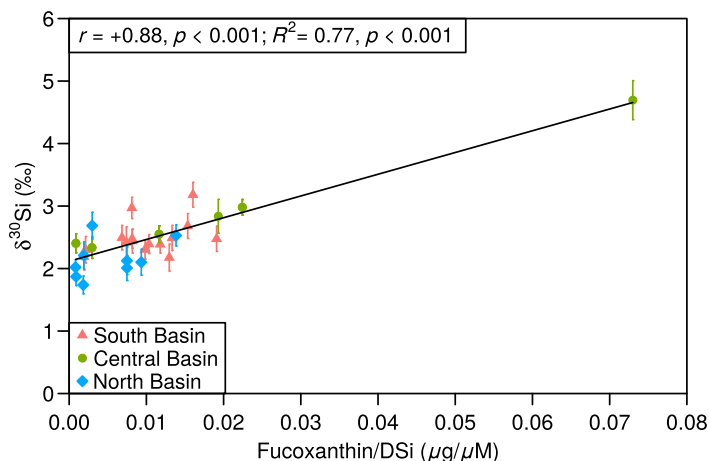


Fig. 7. Fucoxanthin/DSi ($\mu\text{g}/\mu\text{M}$) vs. $\delta^{30}\text{Si}_{\text{DSi}}$ (‰) for data from all of the Lake Baikal sites. A regression trend line and significant correlation coefficients are also provided (refer to Table 1). Respective $\delta^{30}\text{Si}_{\text{DSi}}$ analytical uncertainties are also displayed (2σ ; as cited in Supporting Information Table S1). Only data above the DCM and the applied photic zone cutoff of 20 m were selected, to capture the zone of highest productivity ($n = 30$). South (orange triangles), central (green circles), and north (blue diamonds) basin sites are all differentiated. [Color figure can be viewed at wileyonlinelibrary.com]

isotope data in the central basin will be discussed in “Tracing ‘*Aulacoseira* bloom years’ in Lake Baikal” and “Quantifying sub-surface DSi utilization at central basin sites in Lake Baikal” sections.

The lack of evidence that picocyanobacteria substantially influence DSi uptake in Lake Baikal, corroborates earlier studies that $\delta^{30}\text{Si}_{\text{DSi}}$ acts as a diatom utilization proxy in Lake Baikal (Panizzo et al. 2016, 2017). As such, DSi uptake and the subsequent fractionation of DSi during diatom bloom development, predominantly occurs during spring (May–June) months and the legacy of this is recorded in summer, stratified waters (presented in this study). An increase in the heavier ^{30}Si isotope composition of the dissolved pool therefore occurs through the progressive utilization of the lighter ^{28}Si isotope by diatoms (the dominant spring primary producers in Lake Baikal) leading to the progressive enrichment of the isotopic composition of surface waters (in the absence of DSi supply), manifested by a strong negative correlation between DSi and $\delta^{30}\text{Si}_{\text{DSi}}$ (Table 1; Fig. 6). This finding is corroborated by Panizzo et al. (2016) where $\delta^{30}\text{Si}_{\text{diatom}}$ signatures showed a progressive enrichment from $+0.67\text{‰}$ (May 2012) to $+1.37\text{‰}$ (August 2012), attributed to the progressive enrichment of the lake surface, with spring diatom bloom development.

Spatial patterns of DSi utilization at Lake Baikal

As a result of the findings presented above, we now test the hypotheses that $\delta^{30}\text{Si}_{\text{DSi}}$ approaches can be applied in Lake Baikal to explore evidence of enhanced diatom bloom development as a response to eutrophication (“Evidence for

enhanced algal productivity in Lake Baikal” section) (Kravtsova et al. 2014; Kobanova et al. 2016; Timoshkin et al. 2016). We also explore the evidence for the presence of an “*Aulacoseira* bloom year” in 2013, in the light of high $\delta^{30}\text{Si}_{\text{DSi}}$ signatures in the central region of Lake Baikal (“Tracing ‘*Aulacoseira* bloom years’ in Lake Baikal” section).

Evidence for enhanced algal productivity in Lake Baikal

DCM often develop during the summer in deep transparent oligotrophic lakes due to photoacclimation for non-motile phytoplankton. Some of the reasons for these layers are to avoid photoinhibition via photosynthetically active radiation and ultraviolet radiation (e.g., Sommaruga 2001; Modenutti et al. 2013). While photoadaptation of phytoplankton can be an important driver in determining the depth of DCM (White and Matsumoto 2012), greater nutrient availability at depth is also argued to be central (Saros et al. 2005). However, eutrophication can cause DCM to shift toward the surface as nutrient availability increases and light availability is restricted through algal self-shading (Klausmeier and Litchman 2001; Zhang et al. 2012). August 2013 Chl *a* surveys from Lake Baikal suggest that DCM peaks are shallower and less defined in the south (than the central and north) basin, with algal biomass distributed throughout the surface waters, alongside the highest surface-water $\delta^{30}\text{Si}_{\text{DSi}}$ signatures and algal pigment concentrations (Figs. 2a–c, 3, 4a–c). In contrast, one south basin site (BAIK13-10) has a deeper DCM and decreasing trend (although within AU) in $\delta^{30}\text{Si}_{\text{DSi}}$ signatures between 50 m and the surface (Fig. 3). Surface-water $\delta^{30}\text{Si}_{\text{DSi}}$ compositions at this site fall within the range of those reported for other south basin locations (Panizzo et al. 2017) (Supporting Information Table S1). However, due to its close proximity to the Selenga Delta (c. 10 km), and its shallower water depth, it is possible that inflowing waters from the Selenga River, which account for up to 62% of total inflowing waters (Seal and Shanks 1998; Fig. 1) and assimilate with Baikal lake waters c. 5–7 km from the shoreline (Sorokovikova et al. 2012), may account for the distinctive profile at depth. For example, river waters deliver nutrients, which lead to turbulent deeper water column mixing at BAIK13-10, thus accounting for the increasing trend at depth (50 m) in isotopic compositions and deeper DCM.

North basin sites have nutrient and algal biomass profiles, which indicate more oligotrophic conditions. DCM are deeper in the north basin sites (Fig. 3) and is coincident with the higher $\delta^{30}\text{Si}_{\text{DSi}}$ compositions, indicating a deeper algal production zone (Fig. 2c). Estimates of spring diatom surface-water DSi export are greater in south basin (between 29% and 91%) than in the central (between 38% and 70%) and north (between -2% and 51%) basins (Panizzo et al. 2017). This lower surface diatom nutrient utilization (and export) is a result of the prolonged ice cover duration in north basin sites (over south and central basin locations), and

therefore the decreased spring bloom duration, in addition to the more oligotrophic conditions in the north of Lake Baikal.

It is commonly accepted that increasing lake surface temperature trends have driven pelagic phytoplankton successional changes at Lake Baikal (Izmest'eva et al. 2016), and recently eutrophication (which has been detected in shallow regions of the lake; Kobanova et al. 2016) has also been considered to have an effect on phytoplankton compositions (Fietz et al. 2005a). Our data highlight the spatial differences in Lake Baikal algal productivity (e.g., greater in south basin upper waters). There is little in our data to suggest that these south and north basin patterns are driven by eutrophication in the pelagic areas, especially given the occurrence for a high diatom bloom event in 2013 ("Tracing 'Aulacoseira bloom years' in Lake Baikal" section). However, the distinct algal pigment and $\delta^{30}\text{Si}_{\text{DSi}}$ signature profiles from central basin locations (including Maloe More) are quite distinct from this longitudinal productivity gradient at Lake Baikal and reasons accounting for this (a probable "Aulacoseira bloom year" year and nutrient loading) are discussed below.

Tracing "Aulacoseira bloom years" in Lake Baikal

Pigment, isotopic data, and relationships among them in central basin (BAIK13-12; Fig. 1) and Maloe More (sites BAIK13-13 and 14; Fig. 1) are very different from other parts of the lake. For example, DCM are deeper (20–34 m) and coincident with the base of the photic zone (35–43 m) and maxima in zeaxanthin, fucoxanthin and $\delta^{30}\text{Si}_{\text{DSi}}$ signatures are observed. These observations are consistent with a deeper diatom bloom (as demonstrated by central basin $\delta^{30}\text{Si}_{\text{DSi}}$ and fucoxanthin/DSi correlations: $r = 0.99$, $p < 0.001$; Table 1), due to the deeper photic zone depths of the central basin and higher nutrient availability at depth (Jewson et al. 2010).

Under ice monitoring in spring 2013 also identified a notable *A. baicalensis* bloom in the south basin (E. A. Silow pers. comm.). Our data from the central basin of Lake Baikal support this early evidence of a considerable *A. baicalensis* spring (March) bloom (T. Ozersky pers. comm.) and suggest it expanded from the south basin (where the highest composite $\delta^{30}\text{Si}_{\text{DSi}}$ surface-water signatures are seen [$+2.55 \pm 0.34\text{‰}$, 1 SD]) into the central regions of the lake and possibly into Maloe More. As outlined in "Examining main drivers behind DSi uptake at Lake Baikal" section, we attribute the highest peak in $\delta^{30}\text{Si}_{\text{DSi}}$ signatures at the single pelagic central basin site BAIK13-12 ($+4.69 \pm 0.31\text{‰}$ at 20 m depth), to the legacy effects of a large spring *A. baicalensis* bloom, due to the large peak in fucoxanthin concentrations in the aphotic zone (at 100 m; Fig. 5). Meanwhile, the absence of a significant relationship between fucoxanthin/DSi ratios and $\delta^{30}\text{Si}_{\text{DSi}}$ in south basin sites (Table 1) suggests that our August 2013 sampling was too late to capture the remnants of the earlier, under-ice, spring diatom bloom in situ (E. A. Silow and T. Ozersky pers. comm.) and it had already sunk below 180 m. The lack of such evidence in the

north basin sites, would suggest that an "Aulacoseira bloom year" potentially was not apparent at these sites in 2013 (as can often be the case), although these hypotheses require further phytoplankton cell counts to be fully tested.

With reference to the *A. baicalensis* 3–4 yearly events, the long-term biogeochemical impacts on DSi availability and cycling in Lake Baikal are still unresolved. These species can utilize up to 30 times more silica per cell than other diatom species, for their resting spore formation (a critical under ice stage in their life cycle), which itself is also critically controlled by the duration of ice cover, presence of snow cover and intensity of spring overturn (as detailed in "Phytoplankton succession at Lake Baikal and seasonal nutrient uptake" section) (Jewson et al. 2009, 2010). When sustained *A. baicalensis* blooms develop, they can deplete nutrient availability in surface waters for a number of following years (Shimaraev and Domyshva 2004). Thus, silicon stable isotope approaches may provide a useful means of quantifying seasonal DSi uptake (exhaustion) to more fully explore the implications of the sub-decadal "Aulacoseira bloom years" in Lake Baikal.

Quantifying sub-surface DSi utilization at central basin sites in Lake Baikal

Our results highlight the importance of deeper zones of productivity in the central basin and Maloe More, and thus nutrient uptake estimates can be made based on the higher $\delta^{30}\text{Si}_{\text{DSi}}$ compositions (outside of AU) noted at depth (compared to surface compositions) in these locations of Lake Baikal (Table 2). Sites are excluded where the higher isotopic compositions of profile datasets, at the DCM, fall within AU of surface-water compositions (e.g., BAIK13-10 and BAIK13-18) (Supporting Information Table S1).

We estimate that spring DSi utilization, in central basin sites at the DCM is between 52% and 100%, when applying the parameters set out in Panizzo et al. (2017); assuming an initial DSi composition of $+1.71\text{‰}$ and a diatom fractionation factor of -1.61‰ (Table 2). This corresponds to an estimated DSi utilization of $>100\%$ (e.g., DSi exhaustion) in the pelagic central basin (BAIK13-12) and between 52% and 80% in Maloe More sites (BAIK13-13 and BAIK13-14 at 20 m, respectively; Table 2), which is considerably larger than DSi uptake in surface waters at these locations (between 38% and 70% at these sites; Panizzo et al. 2017). As discussed, we attribute the greater utilization at depth in the pelagic central basin (BAIK13-12), to the progression of an *A. baicalensis* bloom at Lake Baikal, following evidence of south basin spring 2013 data (E. A. Silow pers. comm.) ("Tracing 'Aulacoseira bloom years' in Lake Baikal" section). In particular, these data show that summer deep-water DSi limitation most likely occurred at pelagic site BAIK13-12, following this highly productive diatom spring bloom and was close to occurring at BAIK13-14 (80%; Table 2) in Maloe More.

Table 2. Estimations of percentage DSi utilization by diatoms at zone where peak DCM are at depth (20–30 m) and coincident with peak $\delta^{30}\text{Si}_{\text{DSi}}$ signatures. Calculations are only derived where 20 m $\delta^{30}\text{Si}_{\text{DSi}}$ compositions are greater than surface-water signatures and outside of AU. Surface-water percentage utilization, as calculated by Panizzo et al. (2017) are provided (column denoted with an *), along with percentage diatom utilization at depth, corresponding $\delta^{30}\text{Si}_{\text{DSi}}$ signatures and comparisons made between deeper water productivity zones and the surface (DCM-surface). Data apply a diatom fractionation factor of -1.61‰ , an initial composition of $+1.71\text{‰}$ and an open system model approach (Panizzo et al. 2017).

	Site name	Surface $\delta^{30}\text{Si}_{\text{DSi}}$ utilization* (%)	Peak DCM depth (m)	$\delta^{30}\text{Si}_{\text{DSi}}$ (‰) at DCM c. 20 m	$\delta^{30}\text{Si}_{\text{DSi}}$ (%) utilization at DCM	% difference (DCM -surface)
South basin	BAIK13-1	78	9.9			
	BAIK13-4	48	10.0			
	BAIK13-5	42	10.8			
	BAIK13-7	47	10.1			
	BAIK13-8	44	11.1			
	BAIK13-9	29	15.0			
	BAIK13-10	36	20.6			
	BAIK13-11	91	14.6			
Central basin	BAIK13-12	70	33.9	+4.69	>100	>30
	BAIK13-13	43	20.9	+2.55	52	9
	BAIK13-14	38	19.8	+2.98	80	40
North basin	BAIK13-16	51	14.8			
	BAIK13-17	28	16.0			
	BAIK13-18	16	23.2			
	BAIK13-19	-2	15.1			

As already outlined, sites BAIK13-13, 14 are located in the relatively shallow and more hydrologically restricted Maloe More region of Lake Baikal. This region is also more productive due to localized nutrient loading (as is the case in the eastern shore embayments of Chivyrkuisky and Barguzin; Izmet'eva et al. 2016; Kobanova et al. 2016). Müller et al. (2005) have documented high P concentrations in the bay of Maloe More, which is corroborated by the high abundances of the diatom *Stephanodiscus meyeri*, which has an ecological affinity to P rich waters (meso-eutrophic and eutrophic; Mackay et al. 2003). Later studies have also demonstrated how total phosphorous (TP) concentrations (measured in August 2013) in this region are double those measured previously in pelagic waters (August months between 1995 and 2009) (E. A. Silow unpubl.), further suggesting the effects of localized eutrophication may indeed be seen here. The presence of deep high Chl *a* biomass at Maloe More sites (Fig. 2b) is therefore attributed to enhanced N and/or P availability early on in the growing season, which in turn drives greater DSi utilization at BAIK13-13 (c. 50%) and leads to near exhaustion at BAIK13-14 (80%) (Fig. 1). This pattern was likely enhanced by an *A. baicalensis* bloom in this region, which due to the species' high DSi demand (and the greater availability of N and P), could also seasonally account for near DSi limitation (particularly in the pelagic central site of BAIK13-12) ("Evidence for enhanced algal productivity in Lake Baikal" section).

As outlined in "Phytoplankton succession at Lake Baikal and seasonal nutrient uptake" section, the extent of spring

diatom growth has been found to influence the size of the summer picocyanobacteria blooms, due to the amount of bioavailable phosphorus remaining within the water column (Krivtsov et al. 2000). Contrary to Krivtsov et al. (2000), our data does not support the interpretation of spring DSi exhaustion ("Quantifying sub-surface DSi utilization at central basin sites in Lake Baikal" section), in central and Maloe More sites, leading to a reduction in summer picocyanobacteria populations at Lake Baikal, as measured zeaxanthin concentrations were higher than existing summer measurements from across the lake (Fietz et al. 2005b). Rather, the data suggest a continuous nutrient supply in Maloe More strait (e.g., Müller et al. 2005), as a response to localized eutrophication, which means that nutrients remain replete during the summer (zeaxanthin production). This is most likely a direct response to increasing summer tourism in this embayment region of Lake Baikal over recent decades (Silow 2014), which has been posing an increasing environmental threat (e.g., direct nutrient loading; Timoshkin et al. 2016). Our data demonstrate the potential susceptibility of Maloe More, to the effects of eutrophication in Lake Baikal particularly during large diatom ("*Aulacoseira* bloom") event years. With evidence of a shortening of the ice cover duration in recent decades at Lake Baikal (Todd and Mackay 2003; Hampton et al. 2008), subsequent warmer summer surface waters (Hampton et al. 2008; Shimaraev and Domysheva 2013) and our evidence of potential eutrophication in Maloe More, this fine ecological balance may be disrupted and the

implications for long term DSi availability (and utilization) in Lake Baikal need to be considered.

Conclusions

We present the first combination of summer water column algal pigment concentration and $\delta^{30}\text{Si}_{\text{DSi}}$ data from Lake Baikal to understand the differences in algal biomass across the lake. Algal productivity is heterogeneous across the lake, reflecting the complex interaction between abiotic (e.g., ice off duration, lake water mixing, and nutrient availability) processes in the different basins of the lake. In general, the south basin surface waters have a higher algal biomass, lower DSi concentration, and higher $\delta^{30}\text{Si}_{\text{DSi}}$ composition, when compared to the northern and central basins. In contrast, algal biomass is greatest at depth in the central and northern basins over the south, and the photic zone depth is also greater in these basins. The combined analyses do not support the hypothesis that picocynobacteria are a significant control on DSi uptake, but corroborate that $\delta^{30}\text{Si}_{\text{DSi}}$ may be used as a spring diatom utilization proxy across Lake Baikal sites. Greater DSi utilization occurs at depth (20 m) in central sites with stable isotope modeling approaches estimating this to be c. 10–40% more than diatom utilization in surface waters in 2013. We propose this seasonal increase in deeper water DSi uptake to be a result of a notable *A. baicalensis* bloom in the central region of the lake. High DSi utilization in the Maloe More region is proposed to reflect localized eutrophication, which enhances DSi limitation when N and P availability increases.

References

- Alleman, L. Y., D. Cardinal, C. Cocquyt, P. D. Plisnier, J. P. Descy, I. Kimirei, D. Sinyinza, and L. André. 2005. Silicon isotopic fractionation in Lake Tanganyika and its main tributaries. *J. Great Lakes Res.* **31**: 509–519. doi:10.1016/S0380-1330(05)70280-X
- Baines, S. B., B. S. Twining, M. A. Brzezinski, J. W. Krause, S. Vogt, D. Assael, and H. McDaniel. 2012. Significant silicon accumulation by marine picocyanobacteria. *Nat. Geosci.* **5**: 886–891. doi:10.1038/ngeo1641
- Belykh, O. I., G. Ekaterina, T. Sorokovikova, A. Saphonova, and I. V. Tikhonova. 2006. Autotrophic picoplankton of Lake Baikal: Composition, abundance and structure. *Hydrobiologia* **568**: 9–17. doi:10.1007/s10750-006-0340-8
- Bondarenko, N. A., and V. K. Evstafev. 2006. Eleven and ten year basic cycles of Lake Baikal spring phytoplankton conformed to solar activity cycles. *Hydrobiologia* **568**: 19–24. doi:10.1007/s10750-006-0339-1
- Delvaux, C., D. Cardinal, V. Carbonnel, L. Chou, H. J. Hughes, and L. André. 2013. Controls on riverine $\delta^{30}\text{Si}$ signatures in a temperate watershed under high anthropogenic pressure (Scheldt - Belgium). *J. Mar. Syst.* **128**: 40–51. doi:10.1016/j.jmarsys.2013.01.004
- Diehl, S., S. Berger, R. Ptacnik, and A. Wild. 2002. Phytoplankton, light, and nutrients in a gradient of mixing depths: Field experiments. *Ecology* **83**: 399–411. doi:10.2307/2680023
- Durkin, C. A., J. A. Koester, S. J. Bender, and E. V. Armbrust. 2016. The evolution of silicon transporters in diatoms. *J. Phycol.* **52**: 716–731. doi:10.1111/jpy.12441
- Epstein, E. 1999. Silicon. *Annu. Rev. Plant Physiol. Plant Mol. Biol.* **50**: 641–664. doi:10.1146/annurev.arplant.50.1.641
- Falkner, K. K., and others. 1997. Minor and trace element chemistry of Lake Baikal, its tributaries, and surrounding hot springs. *Limnol. Oceanogr.* **42**: 329–345. doi:10.4319/lo.1997.42.2.0329
- Fietz, S., G. Kobanova, L. Izmet'eva, and A. Nicklisch. 2005a. Regional, vertical and seasonal distribution of phytoplankton and photosynthetic pigments in Lake Baikal. *J. Plankton Res.* **27**: 793–810. doi:10.1093/plankt/fbi054
- Fietz, S., M. Sturm, and A. Nicklisch. 2005b. Flux of lipophilic photosynthetic pigments to the surface sediments of Lake Baikal. *Glob. Planet. Change* **46**: 29–44. doi:10.1016/j.gloplacha.2004.11.004
- Fietz, S., A. Nicklisch, and H. Oberhansli. 2007. Phytoplankton response to climate changes in Lake Baikal during the Holocene and Kazantsevo Interglacials assessed from sedimentary pigments. *J. Paleolimnol.* **37**: 177–203. doi:10.1007/s10933-006-9012-y
- Fontorbe, G., C. L. De La Rocha, H. J. Chapman, and M. J. Bickle. 2013. The silicon isotopic composition of the Ganges and its tributaries. *Earth. Planet. Sci. Lett.* **381**: 21–30. doi:10.1016/j.epsl.2013.08.026
- Frings, P. J., W. Clymans, G. Fontorbe, W. Gray, G. J. Chakrapani, D. J. Conley, and C. De La Rocha. 2015. Silicate weathering in the Ganges alluvial plain. *Earth. Planet. Sci. Lett.* **427**: 136–148. doi:10.1016/j.epsl.2015.06.049
- Georg, R. B., B. C. Reynolds, M. Frank, and A. N. Halliday. 2006. New sample preparation techniques for the determination of Si isotopic compositions using MC-ICPMS. *Chem. Geol.* **235**: 95–104. doi:10.1016/j.chemgeo.2006.06.006
- Hampton, S. E., L. R. Izmet'eva, M. V. Moore, S. L. Katz, B. Dennis, and E. A. Silow. 2008. Sixty years of environmental change in the world's largest freshwater lake - Lake Baikal, Siberia. *Glob. Chang. Biol.* **14**: 1947–1958. doi:10.1111/j.1365-2486.2008.01616.x
- Hampton, S. E., D. K. Gray, L. R. Izmet'eva, M. V. Moore, and T. Ozersky. 2014. The rise and fall of plankton: Long-term changes in the vertical distribution of algae and grazers in Lake Baikal, Siberia. *PLoS One* **9**: e88920. doi:10.1371/journal.pone.0088920
- Hohmann, R., R. Kipfer, F. Peeters, G. Piepke, D. M. Imboden, and M. N. Shimaraev. 1997. Deep-water renewal in Lake Baikal. *Limnol. Oceanogr.* **42**: 841–855. doi:10.4319/lo.1997.42.5.0841
- Hughes, H. J., S. Bouillon, L. André, and D. Cardinal. 2012. The effects of weathering variability and anthropogenic

- pressures upon silicon cycling in an intertropical watershed (Tana River, Kenya). *Chem. Geol.* **308–309**: 18–25. doi:10.1016/j.chemgeo.2012.03.016
- Hughes, H. J., F. Sondag, R. V. Santos, L. André, and D. Cardinal. 2013. The riverine silicon isotope composition of the Amazon Basin. *Geochim. Cosmochim. Acta* **121**: 637–651. doi:10.1016/j.gca.2013.07.040
- Izmet'eva, L. R., and others. 2016. Lake-wide physical and biological trends associated with warming in Lake Baikal. *J. Great Lakes Res.* **42**: 6–17. doi:10.1016/j.jglr.2015.11.006
- Jeppesen, E., and others. 2011. Zooplankton as indicators in lakes: A scientific-based plea for including zooplankton in the ecological quality assessment of lakes according to the European Water Framework Directive (WFD). *Hydrobiologia* **676**: 279–297. doi:10.1007/s10750-011-0831-0
- Jewson, D. H., N. G. Granin, A. A. Zhdanov, and R. Y. Gnatovsky. 2009. Effect of snow depth on under-ice irradiance and growth of *Aulacoseira baicalensis* in Lake Baikal. *Aquat. Ecol.* **43**: 673–679. doi:10.1007/s10452-009-9267-2
- Jewson, D. H., N. G. Granin, A. A. Zhdanov, L. A. Gorbunova, and R. Y. Gnatovsky. 2010. Vertical mixing, size change and resting stage formation of the planktonic diatom *Aulacoseira baicalensis*. *Eur. J. Phycol.* **45**: 354–364. doi:10.1080/09670262.2010.492915
- Katz, S. L., L. R. Izmet'eva, S. E. Hampton, T. Ozersky, K. Shchapov, M. V. Moore, S. V. Shimaraeva, and E. A. Silow. 2015. The “Melosira years” of Lake Baikal: Winter environmental conditions at ice onset predict under-ice algal blooms in spring. *Limnol. Oceanogr.* **60**: 1950–1964. doi:10.1002/lno.10143
- Klausmeier, C. A., and E. Litchman. 2001. Algal games: The vertical distribution of phytoplankton in poorly mixed water columns. *Limnol. Oceanogr.* **46**: 1998–2007. doi:10.4319/lno.2001.46.8.1998
- Kobanova, G. I., V. V. Takhteev, O. O. Rusanovskaya, and M. A. Timofeyev. 2016. Lake Baikal ecosystem faces the threat of eutrophication. *Int. J. Ecol.* **2016**: 1. doi:10.1155/2016/6058082
- Kozhov, M. M. 1955. Seasonal and annual changes in the plankton of Lake Baikal [In Russian], p. 133–157. *In* Proceedings of the All-Union Hydrobiological Society, **6**.
- Kozhova, O. M. 1960. About periodical changes in the development of phytoplankton in Lake Baikal [In Russian], p. 28–43. *In* Proceedings of the All-Union Hydrobiological Society, **11**.
- Kozhova, O. M., and L. R. Izmet'eva. 1998. Lake Baikal, evolution and diversity. *Backhuys*.
- Krause, J. W., M. A. Brzezinski, S. B. Baines, J. L. Collier, B. S. Twining, and D. C. Ohnemus. 2017. Picoplankton contribution to biogenic silica stocks and production rates in the Sargasso Sea. *Global Biogeochem. Cycles* **31**: 762–774. doi:10.1002/2017GB005619
- Kravtsova, L. S., and others. 2014. Nearshore benthic blooms of filamentous green algae in Lake Baikal. *J. Great Lakes Res.* **40**: 441–448. doi:10.1016/j.jglr.2014.02.019
- Krivtsov, V., E. Bellinger, D. Sigee, and J. Corliss. 2000. Interrelations between Si and P biogeochemical cycles - a new approach to the solution of the eutrophication problem. *Hydrol. Process.* **14**: 283–295. doi:10.1002/(SICI)1099-1085(20000215)14:2<283::AID-HYP926>3.0.CO;2-9
- Krivtsov, V., E. G. Bellinger, and D. C. Sigee. 2005. Elemental composition of *Mycrocystis aeruginosa* under conditions of lake nutrient depletion. *Aquat. Ecol.* **39**: 123–134. doi:10.1007/s10452-004-6833-5
- Mackay, A. W., R. W. Battarbee, R. J. Flower, N. G. Granin, D. H. Jewson, D. B. Ryves, and M. Sturm. 2003. Assessing the potential for developing internal diatom-based transfer functions for Lake Baikal. *Limnol. Oceanogr.* **48**: 1183–1192. doi:10.4319/lo.2003.48.3.1183
- McGowan, S., P. Barker, E. Y. Haworth, P. R. Leavitt, S. C. Maberly, and J. Pates. 2012. Humans and climate as drivers of algal community change in Windermere since 1850. *Freshw. Biol.* **57**: 260–277. doi:10.1111/j.1365-2427.2011.02689.x
- Modenutti, B., E. Balseiro, M. B. Navarro, C. Laspoumaderes, M. S. Souza, and F. Cuassolo. 2013. Environmental changes affecting light climate in oligotrophic mountain lakes: The deep chlorophyll maxima as a sensitive variable. *Aquat. Sci.* **75**: 361–371. doi:10.1007/s00027-012-0282-3
- Moore, M. V., S. E. Hampton, L. R. Izmet'yeva, E. A. Silow, E. V. Peshkova, and B. K. Pavlov. 2009. Climate change and the world's “Sacred Sea” - Lake Baikal, Siberia. *BioScience* **59**: 405–417. doi:10.1525/bio.2009.59.5.8
- Moss, B., and others. 2011. Allied attack: Climate change and eutrophication. *Inland Waters* **1**: 101–105. doi:10.5268/IW-1.2.359
- Müller, B., M. Maerki, M. Schmid, E. G. Vologina, B. Wehrli, A. Wüest, and M. Sturm. 2005. Internal carbon and nutrient cycling in Lake Baikal: Sedimentation, upwelling, and early diagenesis. *Glob. Planet. Chang.* **46**: 101–124. doi:10.1016/j.gloplacha.2004.11.008
- Nagata, T., and others. 1994. Autotrophic picoplankton in southern Lake Baikal - abundance, growth and grazing mortality during summer. *J. Plankton Res.* **16**: 945–959. doi:10.1093/plankt/16.8.945
- Nelson, D. M., G. F. Riedel, R. Millan-Nunez, and J. R. Lara-Lara. 1984. Silicon uptake by algae with no known Si requirement. 1. True cellular uptake and pH-induced precipitation by *Phaeodactylum tricorutum* (Bacillariophyceae) and *Platymonas* sp. (Prasinophyceae). *J. Phycol.* **20**: 141–147. doi:10.1111/j.0022-3646.1984.00141.x
- O'Donnell, D. R., P. Wilburn, E. A. Silow, L. Y. Yampolsky, and E. Litchman. 2017. Nitrogen and phosphorous colimitation of phytoplankton in Lake Baikal: Insights from a spatial survey and nutrient enrichment experiments. *Limnol. Oceanogr.* **62**: 1383–1392. doi:10.1002/lno.10505

- Opfergelt, S., E. S. Eiriksdottir, K. W. Burton, A. Einarsson, C. Siebert, S. R. Gislason, and A. N. Halliday. 2011. Quantifying the impact of freshwater diatom productivity on silicon isotopes and silicon fluxes: Lake Myvatn, Iceland. *Earth Planet. Sci. Lett.* **305**: 73–82. doi:10.1016/j.epsl.2011.02.043
- O'Reilly, C. M., and others. 2015. Rapid and highly variable warming of lake surface waters around the globe. *Geophys. Res. Lett.* **42**: 10773–10781. doi:10.1002/2015GL066235
- Panizzo, V. N., G. E. A. Swann, A. W. Mackay, E. Vologina, M. Sturm, V. Pashley, and M. S. A. Horstwood. 2016. Insights into the transfer of silicon isotopes into the sediment record. *Biogeosciences* **13**: 147–157. doi:10.5194/bg-13-147-2016
- Panizzo, V. N., G. E. Swann, A. W. Mackay, E. G. Vologina, V. H. Pashley, and M. S. A. Horstwood. 2017. Constraining modern-day silicon cycling in Lake Baikal. *Global Biogeochem. Cycles* **31**: 556–574. doi:10.1002/2016GB005518
- Peeters, F., R. Kipfer, R. Hohmann, M. Hofer, D. M. Imboden, G. G. Kodenev, and T. Khozder. 1997. Modeling transport rates in Lake Baikal: Gas exchange and deep water renewal. *Environ. Sci. Technol.* **31**: 2973–2982. doi:10.1021/es9700459
- Pondaven, P., O. Ragueneau, P. Treguer, A. Hauvespre, L. Dezileau, and J. L. Reyss. 2000. Resolving the 'opal paradox' in the Southern Ocean. *Nature* **405**: 168–172. doi:10.1038/35012046
- Popovskaya, G. I. 2000. Ecological monitoring of phytoplankton in Lake Baikal. *Aquat. Ecosyst. Health Manag.* **3**: 215–225. doi:10.1080/14634980008657017
- Popovskaya, G. I., M. V. Usol'tseva, V. M. Domyshcheva, M. V. Sakirko, V. V. Blinov, and T. V. Khodzher. 2015. The spring phytoplankton in the pelagic zone of Lake Baikal during 2007–2011. *Geogr. Nat. Resour.* **36**: 253–262. doi:10.1134/S1875372815030051
- Reynolds, B. C., and others. 2007. An inter-laboratory comparison of Si isotope reference materials. *J. Anal. At. Spectrom.* **22**: 561–568. doi:10.1039/B616755A
- Saros, J. E., S. J. Interlandi, S. Doyle, T. J. Michel, and C. E. Williamson. 2005. Are the deep chlorophyll maxima in alpine lakes primarily induced by nutrient availability, not UV avoidance? *Arct. Antarct. Alp. Res.* **37**: 557–563. doi:10.1657/1523-0430(2005)037[0557:ATDCMI]2.0.CO;2
- Satoh, Y., and others. 2006. Nutrient limitation of the primary production of phytoplankton in Lake Baikal. *Limnology* **7**: 225–229. doi:10.1007/s10201-006-0187-8
- Schultze-Lam, S., G. Harauz, and T. J. Beveridge. 1992. Participation of cyanobacterial S layer formation in fine-grain mineral formation. *J. Bacteriol.* **174**: 7971–7981. doi:10.1128/jb.174.24.7971-7981.1992
- Seal, R., and W. Shanks. 1998. Oxygen and hydrogen isotope systematics of Lake Baikal, Siberia: Implications for paleoclimate studies. *Limnol. Oceanogr.* **43**: 1251–1261. doi:10.4319/lo.1998.43.6.1251
- Sherstyankin, P. P., S. P. Alekseev, A. M. Abramov, K. G. Stavrov, M. De Batist, R. Hus, M. Canals, and J. L. Casamor. 2006. Computer-based bathymetric map of Lake Baikal. *Dokl. Akad. Nauk.* **408**: 564–569. doi:10.1134/S1028334X06040131
- Shimaraev, M. N. 1971. Hydrometeorological factors and variation in the abundance of Baikal plankton [In Russian], p. 259–267. In N. A. Florensov, and B. F. Lut [eds.], *Limnology of Deltaic Regions of Lake Baikal*. Nauka, Leningrad.
- Shimaraev, M. N., V. I. Verbolov, N. G. Granin, and P. P. Sherstyankin. 1994. Physical limnology of Lake Baikal: A review, p. 1–89. Baikal International Centre for Ecological Research, Irkutsk.
- Shimaraev, M. N., and V. M. Domyshcheva. 2004. Climate and long-term silica dynamics in Lake Baikal. *Russ. Geol. Geophys.* **45**: 310–316.
- Shimaraev, M. N., E. S. Troitskaya, V. V. Blinov, V. G. Ivanov, and R. Y. Gnatovskii. 2012. Upwellings in Lake Baikal. *Dokl. Akad. Nauk.* **442**: 272–700. doi:10.1134/S1028334X12020183
- Shimaraev, M. N., and V. M. Domyshcheva. 2013. Trends in hydrological and hydrochemical processes in Lake Baikal under conditions of modern climate change, p. 43–66. In C. R. Goldman, M. Kumagi, and R. D. Roberts [eds.], *Climatic change and global warming of inland waters*. John Wiley and Sons.
- Sigeo, D. C., and Levado, E. 2000. Cell surface elemental composition of *Microcystis aeruginosa*: High-Si and low-Si subpopulations within the water column of a eutrophic lake. *J. Plankt. Res.* **22**: 2137–2153.
- Silow, E. A. 2014. Lake Baikal: Current environmental problems, p. 1–9. In S. E. Jørgensen [ed.], *Encyclopedia of environmental management*. New York: Taylor and Francis.
- Sommaruga, R. 2001. The role of solar UV radiation in the ecology of alpine lakes. *J. Photochem. Photobiol. B* **62**: 35–42. doi:10.1016/S1011-1344(01)00154-3
- Sorokovikova, L. M., and others. 2012. Plankton composition and water chemistry in the mixing zone of the Selenga River with Lake Baikal. *Hydrobiologia* **695**: 329–341. doi:10.1007/s10750-012-1200-3
- Timoshkin, O. A., and others. 2016. Rapid ecological change in the coastal zone of Lake Baikal (East Siberia): Is the site of the world's greatest freshwater biodiversity in danger? *J. Great Lakes Res.* **42**: 487–497. doi:10.1016/j.jglr.2016.02.011
- Todd, M. C., and A. W. Mackay. 2003. Large-scale climatic controls on Lake Baikal ice cover. *J. Clim.* **16**: 3186–3199. doi:10.1175/1520-0442(2003)016<3186:LCCOLB>2.0.CO;2
- Weiss, R. F., E. C. Carmack, and V. M. Koropalov. 1991. Deep-water renewal and biological production in Lake Baikal. *Nature* **349**: 665–669. doi:10.1038/349665a0
- White, B., and K. Matsumoto. 2012. Causal mechanisms of the deep chlorophyll maximum in Lake Superior: A

- numerical modeling investigation. *J. Great Lakes Res.* **38**: 504–513. doi:10.1016/j.jglr.2012.05.001
- Zhang, Z., X. Q. He, and Z. Zhang. 2012. Eutrophication status, mechanisms and its coupling effect with algae blooming in Bohai. *Mar. Environ. Sci.* **4**: 465–468.
- Zhang, A. Y., J. Zhang, J. Hu, R. F. Zhang, and G. S. Zhang. 2015. Silicon isotopic chemistry in the Changjiang Estuary and coastal regions: Impacts of physical and biogeochemical processes on the transport of riverine dissolved silica. *J. Geophys. Res. Oceans* **120**: 6943–6957. doi:10.1002/2015JC011050

Acknowledgments

The authors would like to thank Mike Sturm (EAWAG), Nikolaj M. Budnev (Irkutsk State University), the captain and crew of the Geolog research boat and Dmitry Gladkochub (IEC) in facilitating and organizing all Russian fieldwork. Thanks also go to Alison Ball and Julia Lehman (from Urban Promise Academy in Oakland) who joined our expedition

to help on-board the “Geolog.” In addition, thanks are extended to Simon Chenery and Thomas Barlow (BGS) for ICP-MS analyses of dissolved silicon concentrations. We extend our gratitude to Eugene Silow (Irkutsk State University) and Ted Ozersky (University of Minnesota Duluth) along with their colleagues for their special communications with regards to their preliminary *A. baicalensis* data from spring-summer 2013 sampling. This work was supported by the Natural Environment Research Council [grant numbers NE/J00829X/1, NE/J010227/1, NE/J007765/1].

Conflict of Interest

None declared.

Submitted 03 August 2017

Revised 20 November 2017

Accepted 25 January 2018

Associate editor: Stephanie Hampton